Electronic Supplementary Material (ESI) for ChemComm.
This journal is © The Royal Society of Chemistry 2021

Supporting Information

A bimodal-pore strategy for synthesis of Pt_3Co/C electrocatalyst toward oxygen reduction reaction

Wei Hong,[a] Xinran Shen,[a] Fangzheng Wang,[a] Xin Feng,[b] Jing Li*[a] and Zidong Wei*[a]

[a]*School of Chemistry and Chemical Engineering, Chongqing University, Shapingba 174, Chongqing 400044, China. E-mail: lijing@cqu.edu.cn; zdwei@cqu.edu.cn*

[b]*School of Materials Science and Engineering, Chongqing University, Shapingba 174, Chongqing 400044, China*

Experimental Section

Synthesis of SiO_2/C

0.4 g resorcinol and 1.2 g CTAB were mixed with 12 mL ethanol and 48 mL deionized water to form a uniform solution, into which 0.4 mL 28% ammonia solution and 0.56 mL formaldehyde were further introduced. Several minutes later, the original clear solution becomes a milk-like solution, indicating formation of an emulsion solution. After adding 2 mL TEOS into the solution and continuously stirring it for 24 h at room temperature, the solution was transferred into a 100 mL Teflon-lined autoclave to conduct a hydrothermal reaction at 80 °C for 24 h. Finally，the collected precipitate was annealed at 850 °C for 3 h under N_2 flow with a ramp rate of 1 °C min^{-1}.

Synthesis of Pt_3Co/C-O

100 mg SiO_2/C powder, 0.031 mmol H_2PtCl_6 $6H_2O$ and 0.093 mmol $Co(NO_3)_2$ $6H_2O$ were sequentially added into 50 mL deionized water and the obtained solution was continuously stirred for 12 h to allow ion diffusion into the inner pores. After drying and annealing the product at 600 °C for 2 h under H_2/N_2 gas mixture (10 vol% H_2) flow, Pt_3Co alloy nanoparticles would be in-situ formed in the CTAB-templated pores. Finally etching SiO_2 with HF solution and exhaustedly washing the sample with deionized water would lead to the final Pt_3Co/C-O product.

Synthesis of Pt_3Co/C-B

Firstly, etching SiO_2/C powder (100 mg) in HF solution at room temperature would

result in porous carbon C. Then the obtained carbon C, 0.031 mmol H_2PtCl_6 $6H_2O$ and 0.093 mmol $Co(NO_3)_2$ $6H_2O$ were dispersed into 50 mL deionized water and the obtained solution was continuously stirred for 12 h to allow ion diffusion into the inner pores. After drying and annealing the dried powder at 600 °C for 2 h under H_2/N_2 gas mixture (10 vol% H_2) flow, the final Pt_3Co/C-B product can be achieved.

Characterizations

X-ray diffraction (XRD) patterns were obtained on a Rigaku D/Max 2200PC diffractometer with Cu Kα radiation and the scanning rate was 1° min^{-1}. Transmission electron microscopy (TEM) analyses were performed on a Philips Tecnai G2F20 microscope at an voltage of 200 kV. Scanning electron microscope (SEM) images were obtained on a S-4800 HITACHI microscope. Nitrogen sorption isotherms data were obtained on a Micromeritics Gemini VII 2390 analyzer. Before measurements, the catalysts were degassed in vacuo at 140 °C for 6 h. X-ray photoelectron spectrometer (XPS) was operated on a Kratos XSAM800 spectrometer with a monochromatic Al X-ray source (Al KR, 1.4866 keV).

Electrochemical measurements

The electrochemical measurements were recorded by a three-electrode system. A graphite rod was used as counter electrode, the Ag/AgCl (3.0 M KCl) electrode was used as reference electrode and the glassy carbon electrode (0.196 cm^2) with loaded with our catalysts was used as working electrode. All potentials in this work are

converted to a reversible hydrogen electrode (RHE). The homogeneous catalyst ink was prepared by ultrasonically dispersing the as-prepared catalyst powder in a mixed solution containing 10 uL Nafion solution and 1600 uL ethanol for 30 min. Then, 20 uL catalyst ink was deposited onto the glassy carbon electrode and dried naturally at room temperature. The Pt loading of all catalysts was 17.8 ug cm^{-2}.

Before electrochemical tests, all catalysts were first pretreated by cyclic voltammetry (CV) between 0.05 and 1.2 V at 50 mV s^{-1} in N_2-saturated 0.1 M $HClO_4$ for 50 cycles. Electrochemical active surface area (ECSA) was calculated by CO stripping (electro-oxidation of adsorbed CO) method. Oxygen reduction reaction (ORR) polarization curves were conducted in O_2-saturated 0.1 M $HClO_4$ solution with a rotation speed of 1600 rpm and at scan rate of 10 mV s^{-1}. The ORR polarization curves were collected with the current densities corrected by ohmic iR drop compensation. The accelerated durability test (ADT) was conducted at room temperature by CV between 0.6 and 1.1 V at 50 mV s^{-1} in O_2-saturated 0.1 M $HClO_4$ for 10000 CV cycles.

The ECSA was calculated by the following Equation (1):

$$ECSA=Q_{CO}/(0.42* [Pt]) \quad (1)$$

Where Q_{CO} (mC) represents the electro-oxidation of adsorbed CO, 0.42 mC cm^{-2} is the electrical charge for oxidizing a monolayer of CO on Pt, and [Pt] is the loading amount of Pt on the working electrode. The specific kinetic current densities (j_k) associated with the intrinsic activity of the catalysts and can be calculated according the following

Equation (2):

$$j_k = \frac{j_d * j}{j_d - j} \quad (2)$$

Where j represents the measured current density, j_d represents the diffusion limited current density and j_k represents the kinetic current density.

Antiflooding Measurements

The chronopotentiometry curves were measured in O_2-saturated 0.1 M $HClO_4$ solutions using a self-made working electrode at a constant current. Firstly, homogeneous catalyst ink consisting of Nafion, ethanol and catalyst (with mass ratio of Nafion to catalyst = 0.35:1) was deposited onto the carbon paper with Pt loading of 0.075 mg cm^{-2} (area = 1.0 cm^2). The catalyst was dried naturally under ambient condition and loaded into the ring groove of the working electrode. The chronopotentiometry curves were also recorded by a three-electrode system. A carbon rod was used as counter electrode and an Ag/AgCl (3.0 M KCl) was used as reference electrode. O_2 is flowed maintained at 10 mL min^{-1} during test.

MEA Preparation and Testing

The prepared catalysts and commercial Pt/C (20 wt%) were made into fuel cell cathodes to investigate their applicability. Simply, the homogeneous catalyst ink was prepared by ultrasonically dispersing catalyst, ethanol and Nafion. The Nafion content was 35 wt% in the dried catalyst layer. The obtained catalyst ink was then applied onto the surface of carbon paper in an active area of 5.0 cm^2 and dried under ambient condition.

The Pt loading of cathode and anode are 0.060 mg cm^{-2} and 0.080 mg cm^{-2}, respectively. During H_2-O_2 fuel cell testing, both hydrogen and oxygen have a flow rate of 160 mL min^{-1}. The cell temperature was maintained at 80 °C and the back pressure was set at 170 kPa for both H_2 and O_2. For H_2-air fuel cell tests, pure hydrogen has a flow rate of 160 mL min^{-1}, while the air flow rate is 520 mL min^{-1}. The cell temperature was maintained at 80 °C and the back pressure was set at 100 kPa for both H_2 and air. All tests were conducted at full humidification of anode and cathode.

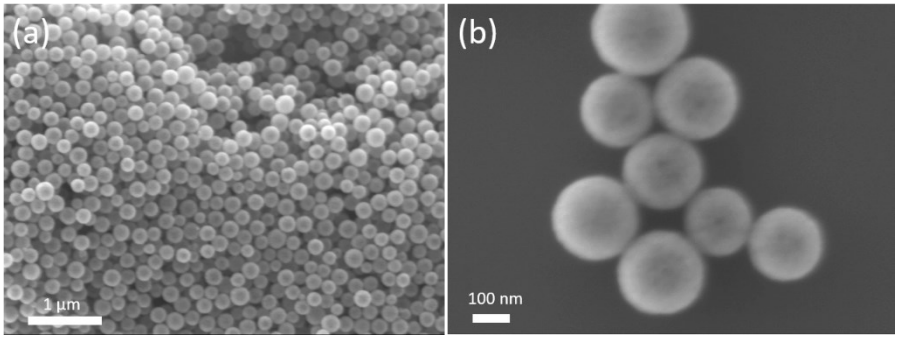

Fig. S1. SEM images of SiO_2/C (a, b)

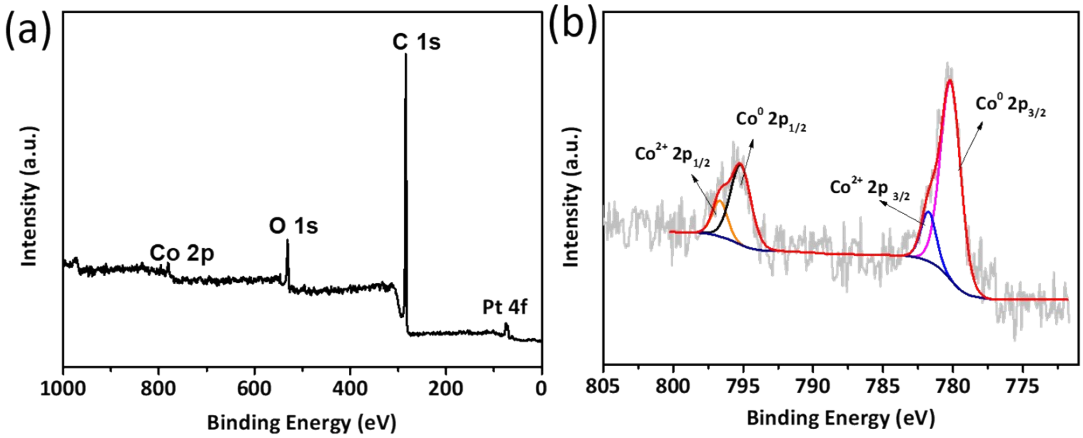

Fig. S2. XPS survey (a) and high-resolution Co 2p spectrum (b) of Pt_3Co/C-O.

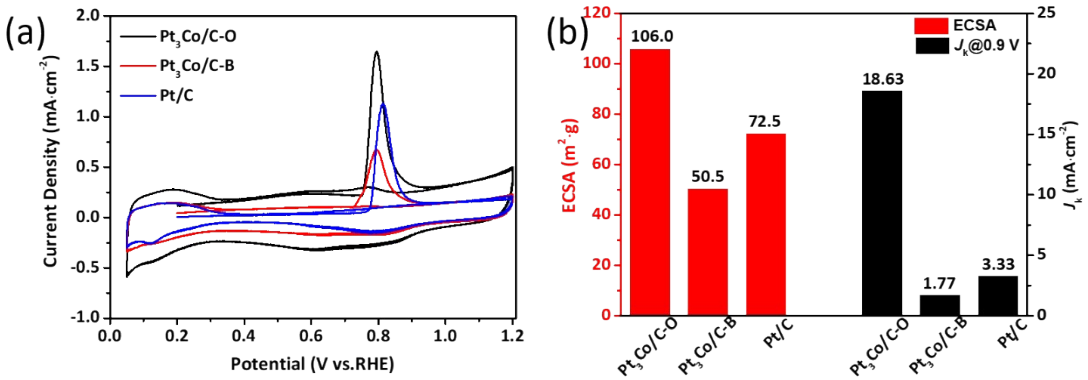

Fig. S3. (a) The CO-stripping curves of Pt/C, Pt_3Co/C-B and Pt_3Co/C-O recorded in CO-saturated 0.1 M $HClO_4$ solution at scan rate of 10 mV s^{-1}; (b) The ECSA and J_k of Pt/C, Pt_3Co/C-B and Pt_3Co/C-O.

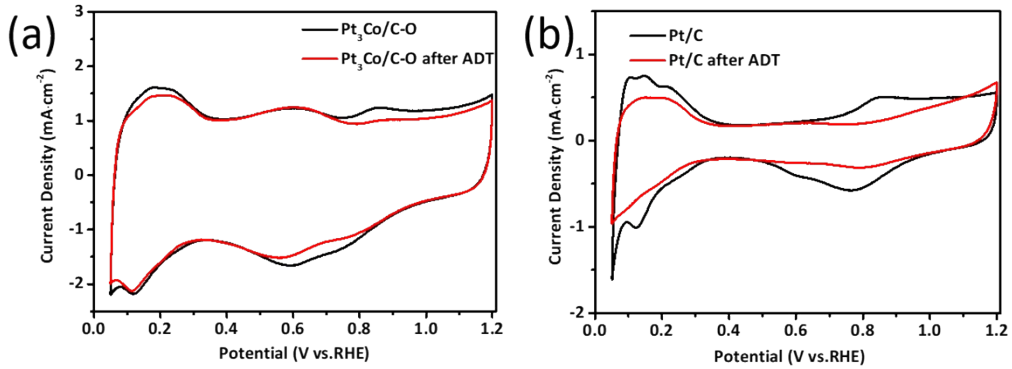

Fig. S4. CV curves of Pt_3Co/C-O (a) and Pt/C (b) catalyst before and after 10 000 potential cycles between 0.6 and 1.1 V versus RHE.

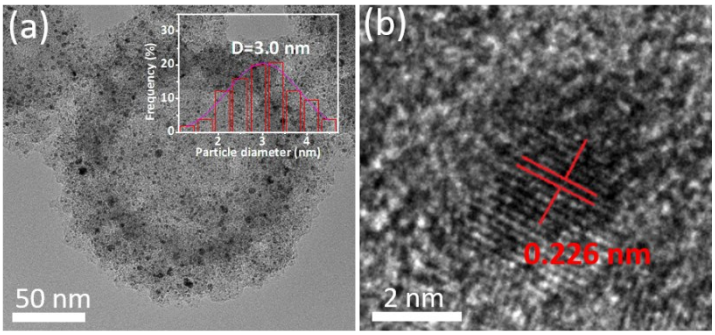

Fig. S5. TEM image (a), particle size distribution (inset) and HRTEM image (b) of Pt_3Co/C-O catalyst after 10000 CV cycles between 0.6 and 1.1 V in O_2-saturated 0.1 M $HClO_4$ at a scan rate of 50 mV s^{-1}.

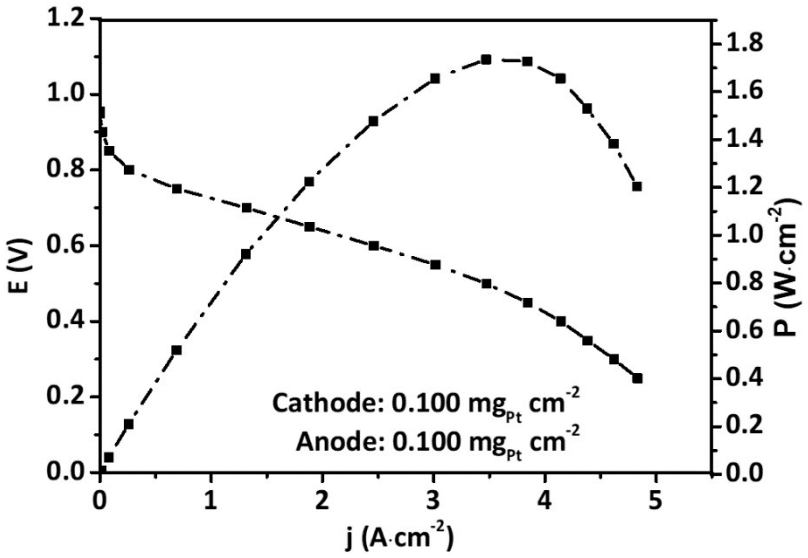

Fig. S6 Polarization curve and power density of H_2-O_2 fuel cell with Pt_3Co/C-O as cathode and Pt/C as anode.

Table S1. Pore parameters of the catalysts.

Sample	S_{BET}[a] ($m^2\ g^{-1}$)	V_t[b] ($cm^3\ g^{-1}$)	V_{micro}[c] ($cm^3\ g^{-1}$)	$V_{meso/macro}$[d] ($cm^3\ g^{-1}$)	D[e] (nm)
SiO_2/C	377.8	0.811	0.022	0.789	2.3
Pt_3Co/C-B	851.4	1.840	0.050	1.790	2~7
Pt_3Co/C-O	804.0	1.809	0.069	1.740	2~9
Pt/C	122.4	1.681	0.0021	1.679	2~10

[a]BET specific surface area.

[b]Total pore volume, $V_t=V_{meso/macro}+V_{micro}$.

[c]t-Plot micropore volume.

[d]BJH adsorption cumulative volume of pores (d＞2 nm).

[e]Pore sizes.

Table S2. Comparisons of the ORR performances at half-cell level.

Catalyst	E_{onset} (V)	$E_{1/2}$ (V)	MA@0.9 V ($A\ mg_{pt}^{-1}$)	Ref
Pt_3Co/C-O	**1.067**	**0.930**	**1.04**	**This work**
Pt_3Co/C-B	**1.014**	**0.847**	**0.10**	**This work**
Ordered $Fe_3Pt/Ti_{0.5}Cr_{0.5}N$	1.03	0.92[a]	0.673	1
Ga-Pt_3Co/C	1.0[a]	0.894	0.75	2
Pd@Pt_{1L} Octahedra	0.98[a]	0.9[a]	0.75	3
Pt-Pd SBCNC	1.05[a]	0.9[a]	0.87	4
$PtCo_3$-H600	1.0[a]	0.9[a]	0.74	5
Pt-o-Cu_3Pt/C	1.03[a]	0.92[a]	0.64	6
PtFeNi	1.02[a]	0.92[a]	0.63	7
O-Pt-Fe@NC/C	1.0[a]	0.9[a]	0.53	8
$L1_0$-FePt/Pt	1.02[a]	0.945	0.7	9
$Pt_{4.8}Fe$/PCNF	0.978	0.824	0.013[a]	10

[a]The data are not given in the literatures, but excavated from the Fig.

Table S3. Comparisons of the ORR performances at MEA-level.

Catalyst	Anode Loading ($mg_{Pt}\ cm^{-2}$)	Cathode Loading ($mg_{Pt}\ cm^{-2}$)	Power Density ($W\ cm^{-2}$)	Current density at 0.6 V ($mA\ cm^{-2}$)	P[a] ($W\ mg_{Pt}^{-1}$)	Ref.
Pt_3Co/C-O	**0.080**	**0.060**	**1.33**	**1780**	**9.5**	**This work**
Pt_3Co/C-B	**0.080**	**0.060**	**0.88**	**1370**	**6.3**	**This work**
Pt_A@Fe_{SA}-N-C	0.130	0.200	1.31	1800	3.97	11
cBCP-PtFe	0.200	0.010	0.92	1300	4.4	12
PtNi/GC-1600 oct	0.200	0.400	0.818	850[b]	1.36	13
PtMg/C	0.120	0.120	1.27	1550[b]	5.3	14
LP@PF-2	0.350	0.035	1.41	1450	3.7	15
PtNi@Pt/C	0.200	0.200	2.40	3100	6.0	16

[a]Peak power density normalized to the Pt loading of the whole cell.

[b]The data are not given in the literatures, but excavated from the H_2-O_2 fuel cell polarization curves.

References

1 Q. Liu, L. Du, G. Fu, Z. Cui, Y. Li, D. Dang, X. Gao, Q. Zheng and J. B. Goodenough, Advanced Energy Materials, 2019, 3, 1803040.

2 M. Li, Z. Zhao, Z. Xia, Y. Yang, M. Luo, Y. Huang, Y. Sun, Y. Chao, W. Yang, W. Yang, Y. Yu, G. Lu and S. Guo, ACS Catalysis, 2020, 5, 3018-3026.

3 M. Zhou, H. Wang, A. O. Elnabawy, Z. D. Hood, M. Chi, P. Xiao, Y. Zhang, M. Mavrikakis and Y. Xia, Chemistry of Materials, 2019, 4, 1370-1380.

4 R. Wu, P. Tsiakaras and P. K. Shen, Applied Catalysis B-Environmental, 2019, 251, 49-56.

5 Z. Wang, X. Yao, Y. Kang, L. Miao, D. Xia and L. Gan, Advanced Functional Materials, 2019, 35, 1902987

6 N. Cheng, L. Zhang, S. Mi, H. Jiang, Y. Hu, H. Jiang and C. Li, ACS Applied Materials & Interfaces, 2018, 44, 38015-38023.

7 H. Kuroki, T. Tamaki, M. Matsumoto, M. Arao, K. Kubobuchi, H. Imai and T. Yamaguchi, Industrial & Engineering Chemistry Research, 2016, 44, 11458-11466.

8 Y. Hu, T. Shen, X. Zhao, J. Zhang, Y. Lu, J. Shen, S. Lu, Z. Tu, H. L. Xin and D. Wang, Applied Catalysis B-Environmental, 2020, 279, 119370.

9 J. Li, Z. Xi, Y.-T. Pan, J. S. Spendelow, P. N. Duchesne, D. Su, Q. Li, C. Yu, Z. Yin, B. Shen, Y. S. Kim, P. Zhang and S. Sun, Journal of the American Chemical Society, 2018, 8, 2926-2932.

10 L. Mao, K. Fu, J. Jin, S. Yang and G. Li, International Journal of Hydrogen Energy, 2019, 33, 18083-18092.

11 X. Ao, W. Zhang, B. Zhao, Y. Ding, G. Nam, L. Soule, A. Abdelhafiz, C. Wang and M. Liu, Energy & Environmental Science, 2020, 13, 3032-3040.

12 J. Choi, Y. J. Lee, D. Park, H. Jeong, S. Shin, H. Yun, J. Lim, J. Han, E. J. Kim, S. S. Jeon, Y. Jung, H. Lee and B. J. Kim, Energy & Environmental Science, 2020, 13, 4921-4929.

13 J. Wang, Q. Xue, B. Li, D. Yang, H. Lv, Q. Xiao, P. Ming, X. Wei and C. Zhang, ACS Applied Materials & Interfaces, 2020, 12, 7047-7056.

14 E. B. Tetteh, H.-Y. Lee, C.-H. Shin, S.-h. Kim, H. C. Ham, T.-N. Tran, J.-H. Jang, S. J. Yoo and J.-S. Yu, ACS Energy Letters, 2020, 5, 1601-1609.

15 L. Chong, J. Wen, J. Kubal, F. G. Sen, J. Zou, J. Greeley, M. Chan, H. Barkholtz, W. Ding and D.-J. Liu, Science, 2018, 362, 1276.

16 J. Choi, J.-H. Jang, C.-W. Roh, S. Yang, J. Kim, J. Lim, S. J. Yoo and H. Lee, Applied Catalysis B-Environmental, 2018, 225, 530-537.